Technical University of Denmark

Description of the Probabilistic Wind Atlas Methodology, Deliverable D3.1

Hahmann, Andrea N.; Witha, Björn; Rife, Daran L.; Frouzakis , Nikolaos; Junk, Constantin; Sile, Tija; Baltscheffsky, Magnus ; Dörenkämper, Martin; Ezber, Yasemin; Bustamante, Elena Garcia ; Gonzalez-Rouco, Fidel; Mentes, Sibel; Navarro, Jorge ; Söderberg, Stefan; Unal, Yurdanur

Publication date:
2017

Document Version
Publisher's PDF, also known as Version of record

Description of the Probabilistic Wind Atlas Methodology
Deliverable D3.1

Edited by: Andrea N. Hahmann
Delivery date: 21 July 2017
Dissemination level: Public

With financial support from NEWA ERA-NET Plus, topic FP7-ENERGY.2013.10.1.2.

Author Information

Name	Organisation	E-mail
Andrea N. Hahmann	DTU, Denmark	ahah@dtu.dk
Björn Witha	ForWind, Germany	bjoern.witha@forwind.de
Daran Rife	DNV-GL, USA	
Nikolaos Frouzakis	ForWind, Germany	
Constantin Junk	ForWind, Germany	
Tija Sile	University of Latvia	
Magnus Baltscheffsky	WeatherTech, Sweden	
Martin Dörenkämper	Fraunhofer IWES, Germany	
Yasemin Ezber	Istanbul Technical Univ.	
Elena Garcia Bustamante	CIEMAT, Spain	
Fidel Gonzalez-Rouco	Univ. Computense Madrid	
Sibel Mentes	Istanbul Technical Univ.	
Jorge Navarro	CIEMAT, Spain	
Stefan Söderberg	WeatherTech, Sweden	
Yurdanur Unal	Istanbul Technical Univ.	

Contents

Executive Summary

A new ensemble method is explored for estimating the uncertainty of the wind resource within Weather Research and Forecasting (WRF) model simulations. The output of the ensemble simulations is processed to create a "map" showing the uncertainty in the wind resource estimate at each geographic location. This new method is demonstrated by performing a collection of 9 different WRF model simulations using combinations of 3 planetary boundary layer schemes, 2 simulation re-initialization strategies, and 2 methods for initializing the land surface state. The results of the simulations are validated against data from 10 meteorological masts in South Africa, part of the Wind Atlas of South Africa (WASA) project, where a long-term set of high-quality observations exist. The results of the ensemble simulations are encouraging, but further analysis is needed to quantify their utility. A key disadvantage of the ensemble simulation strategy employed herein, is that some members may tend to be highly similar to others, leading to overconfidence in the mean and spread of the simulations. Such overconfidence yields misleading estimates of the accuracy, value, and uncertainty of the wind resource.

The results show that we need to develop a method to determine whether any given set of ensemble simulations are statistically distinct (i.e., each simulation provides unique information). Statistically similar ensemble members provide redundant information, falsely increase confidence, and thus should be removed from the set. The next step is also to identify potential statistical techniques (e.g., machine learning) to optimally combine the results from the various ensemble members into a single wind resource map.

We further describe a set of WRF sensitivity simulations for five domains in Europe. These simulations were carried out to determine a few fundamental settings and strategies that are known to have the largest impact on the wind resource. The results of the simulations show consistent systematic differences among the simulations in the various domains.

This report also introduces and explores the applicability of the Analog Ensemble (AnEn) approach, another method to generate uncertainty information of the wind resource. Test results show that the AnEn is well-suited for estimating the long-term wind resource at target sites based on short-term measurements and historical reanalysis model data. A further benefit is that the AnEn technique adds uncertainty information to the long-term wind resource. Preliminary tests with mesoscale model data instead of observations show that the AnEn method could be applied to extend the high-resolution mesoscale wind atlas data set and to provide uncertainty information for the wind atlas data.

Introduction

A wind atlas is associated to the planning phase of wind energy development, which can last several years from strategic spatial planning, to site prospecting, to wind farm design and financing. Detailed and robust information about the relative size of the wind resource across an area is crucial for the commercial evaluation of a wind farm. Today a number of well-established models and methodologies exist for estimating resources and design parameters. These can work well if good local data are available, but the wind energy community is still hampered by projects having large negative discrepancies between calculated and actual resources and design conditions.

This report is divided into three parts. After a brief description of the scope of a wind atlas (section) and mesoscale modeling for wind energy applications (section), we describe in section the probabilistic approach, discuss the results obtained and make recommendations on future work. Section we briefly describe a first sensitivity analysis conducted by various NEWA partners to help ranking the importance of different WRF options in terms of their impact on the variability of variables of interest in different wind climate conditions. Finally in section , we explore the applicability of the Analog Ensemble (AnEn), another method to generate uncertainty information of the wind resource.

1 Wind Atlas Scope

The New European Wind Atlas (NEWA) will provide a unified high-resolution and freely available dataset of wind resource and siting parameters in Europe. Wind statistics will cover onshore Europe and 100 km offshore plus the Baltic and the North Seas (Figure 1), with a horizontal resolution of 20–30 meters at least at 10 wind-turbine relevant heights. The database will be based on at least 10 years of mesoscale simulations at 3 km resolution, with long-term corrections as well as sub-grid microscale corrections to reduce the bias on the local mean wind resource.

In addition to the wind resource information, the new wind atlas will provide information about site suitability conditions (turbulence intensity, wind shear, extreme wind speed), wind variability as well as and wind power predictability from day-ahead to decadal. The predictability

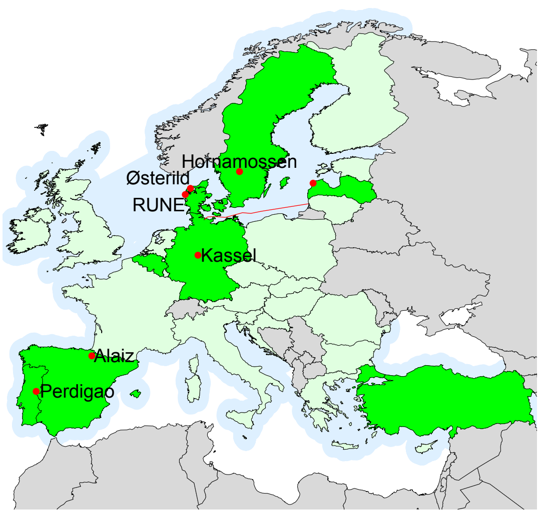

Figure 1. Initial extension of the European domain for the New European Wind Atlas and location of high fidelity experiments.

assessment methodology using climate models is introduced in deliverable D3.2.

Besides variables of immediate use by resource planners, the wind atlas will provide means to feed boundary conditions to microscale models. This will allow not only to improve the wind atlas predictions at local level when better site data becomes available but also to allow a coherent integration with wind farm design tools. Hence, a generalized wind atlas, i.e. free of site effects, will be also part of the NEWA database. Downscaling methodologies with microscale models are introduced in deliverable D3.3.

Integral to the wind atlas methodology is the assessment of the associated uncertainties. The ultimate goal of the wind atlas is to reduce the uncertainties on the assessment of wind resource and the wind conditions that affect the design of wind turbines. To this end, the model-chain will be thoroughly validated across Europe with dedicated experiments and historical wind resource assessment campaigns from industry. The model evaluation strategy is described in deliverable D3.4.

An uncertainty map will calculate the confidence of the wind atlas and, therefore, the intensity to which *in-situ* measurement must be employed before development of a wind farm. The probabilistic wind atlas method examined in this report is the first attempt to such measure.

2 Mesoscale modelling for wind energy applications

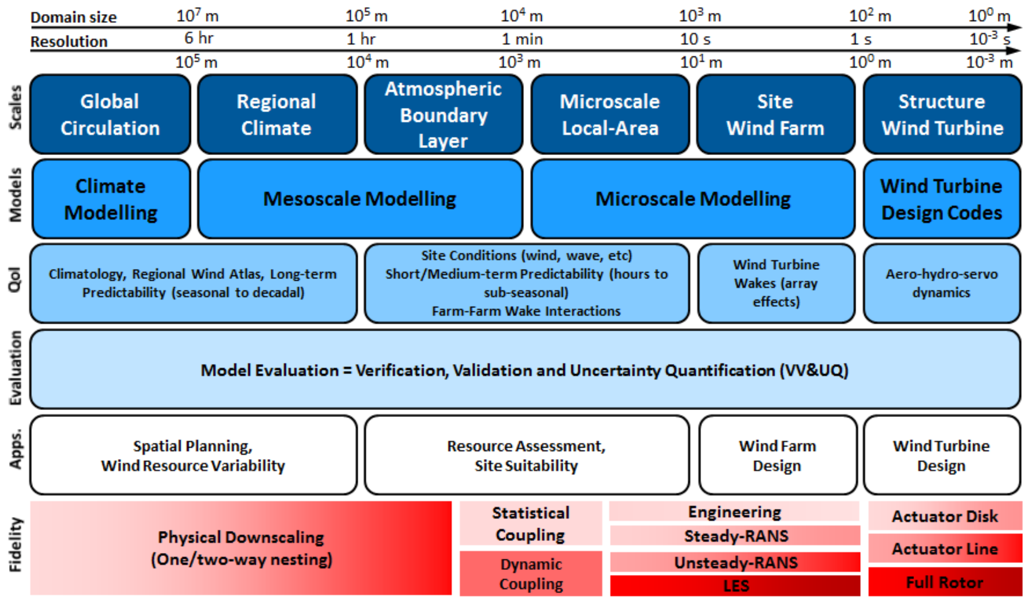

Figure 2. Wind assessment modelling framework indicating typical model scale ranges, relevant outputs for different applications and high-level fidelity levels (the shading indicates the computational cost). Source: (Sanz Rodrigo et al., 2017)

Figure 2 schematically shows the wind assessment model-chain framework with typical scale ranges for each sub-model level and associated applications and flow modeling approaches of various physical fidelity levels (Sanz Rodrigo et al., 2017). Mesoscale models, also called limited-area, cover a limited portion of the planet so they require lateral boundary conditions from a global circulation model (GCM). GCM models use data assimilation to produce the best possible representation of the state of the atmosphere every 3 or 6 hours at horizontal resolutions of several tens of kilometres. These large-scale fields are called analysis in forecasting mode or reanalysis in hindcast mode, when a frozen version of the GCM model is used. For example, the European

Centre for Medium-Range Weather Forecasts (ECMWF) continuously updates the ERA-Interim global reanalysis (Dee et al., 2011a) using a fixed numerical model, released in 2006, that assimilates data since 1979 at approximately 80 km horizontal resolution. The analysis, in contrast, uses the most updated forecasting model to provide the best possible forecast; hence backwards consistency of the data is not satisfied. From a wind atlas perspective we should use reanalysis products as the best guarantee to maintain historical wind climate homogeneity.

Physical downscaling is often done with telescopic nested uniform grids that progressively increase the horizontal resolution down to a few kilometres. This is the case for the Advanced Research WRF (WRF-ARW, where WRF stands for the Weather Research and Forecasting) model, the most widely used open-source mesoscale model (Skamarock et al., 2008). Sub-grid parameterizations are introduced to account for unresolved physics, of which the most relevant for wind is that of the planetary boundary layer (Draxl et al., 2014; Kleczek et al., 2014). Mesoscale models are, in general, not specifically developed for wind energy applications. On the other hand, there is a majority of wind energy meteorologist working with the WRF community model in operational as well as research conditions. The initial objective of the mesoscale group in NEWA is to gather best practices on using WRF for wind resource assessment to come up with a unified modeling methodology. A reference model facilitates the process of "speaking the same language", a fundamental objective for the interpretation of simulation objectives and results.

3 Probabilistic Approach

Numerical wind atlas methodologies have been devised to facilitate estimating wind energy resources over large areas, since it is not possible to blanket the entire project with wind measurement masts. The wind atlas is a database that contains wind statistics (e.g., wind speed distributions) per wind direction and height above ground level often on a regular grid covering a large geographic area.

The method developed at DTU Wind Energy, and used in many wind atlas projects, uses the Weather Research and Forecasting (WRF) model in a dynamical downscaling mode to produce mesoscale analysis. The method has recently been documented in Hahmann et al. (2015) and verified against tall masts in the North and Baltic Sea. The same method was used and verified against measurements in the recent Wind Atlas for South Africa (Hahmann et al., 2014).

Numerical wind atlases are validated against measurements from tall wind masts. The validation errors are useful to assess the possible errors around the observation sites. However, because of their limited number the measurement masts only sample the large variety of wind climates and terrains across a given area providing an illustration of the range of errors and uncertainties that generally would be expected at similar sites. Away from these sites, it is not straightforward to estimate the possible errors in wind resource assessments made from the wind atlas, in particular at sites that are either far from validation masts or at sites of a different wind climate or topography.

In an analogous way to what is done in Numerical Weather Prediction (NWP) and climate prediction, we explore the possibility to estimate the uncertainty of the wind resource estimate based on and ensemble of WRF simulations. These ensemble simulations are created by runs with different physical parameterizations or by introducing variations in the initial atmosphere and surface conditions. The results of the ensemble simulations can be processed to give a “map” of the spread of the wind resource estimation. By comparing these “maps” with the observed wind resources at the sites and by relating these to the terrain complexity and wind climate complexity, it might be possible to diagnose the geographic distribution of possible errors in the wind resources away from the observation sites.

3.1 Ensembles in NWP

Early in the 20th century it was recognized that small uncertainties in the initial conditions or the prediction model will develop over time to meso- and synoptic-scale errors, and thus the predictability of the detailed weather evolution is limited (Lorenz, 1969). In NWP an objective way to estimate the uncertainty of the forecast is to run an ensemble prediction system, which provides a probabilistic forecast of the atmospheric evolution (Berner et al., 2011).

To account for initial condition error, it is common practice to start each member of the ensemble from slightly different initial conditions, but in generating such set of initial conditions one must attempt to perturb the model in directions that will exhibit maximal error growth. However, even with the standard operational methods, ensemble forecasts tend to be underdispersive and underestimate the true uncertainty of the model evolution (Buizza et al., 2005).

Another major contribution to the forecast uncertainty is the model error, from either parameter and parameterisation uncertainty, or altogether unrepresented subgrid-scale processes (Berner et al., 2011). The errors that arise from a misrepresentation of subgrid-scale processes can affect both the variability and the mean error of a model. But contrary to the initial condition approach, there is no unique method to represent these errors in an ensemble prediction system. The suggested approaches are: stochastic dynamic models (Palmer, 2001), multiple physics schemes (e.g. Lee et al., 2012), or parameter variations in the physics schemes (Stainforth et al., 2005).

3.2 Ensembles in climate prediction

In long-term climate prediction, where exact prediction of the time evolution of the atmosphere is not of vital importance, ensemble simulations are being used to sample structural model uncertainties arising from choices such as resolution, the set of processes included in the model and the basic assumptions on which its parametrisations are based (Murphy et al., 2004). This approach is the standard in current Intergovernmental Panel on Climate Change reports (e.g. IPCC, 2013).

3.3 Ensembles in dynamical downscaling

Ensemble simulations are also used in the context of dynamical downscaling from an ensemble of global model predictions, e.g. CORDEX (Giorgi et al., 2009). The divergence of ensemble model results provides an indication of the range of uncertainty if it is not known which of the models forming the ensemble are more reliable; however, it does not properly describe probabilities of the possible outcome because the ensemble of models does not constitute a valid statistical sample (Takayabu et al., 2016).

The setup for the simulations used in dynamical downscaling for wind resource assessment are in the intersection of NWP and traditional dynamical downscaling. The simulations are reinitialized often (1–10 days), but in most instances we are interested in their skill in representing the spatial and temporal distribution of wind speed and not the exact match between each simulated and observed instance (Hahmann et al., 2015).

In a recent paper, Al-Yahyai et al. (2012) used an “ensemble” approach to simulate the wind speed climatology over Oman. They used an ensemble of four simulations with two large scale forcings and two regional models. They conclude that “The results proved the effectiveness for the proposed approach and showed that the Ensemble Mean Approach performed better in average than the Individual Members Approach.” However, in their context, the ensemble mean just smooths out the details of each individual ensemble member. In the context of forecasting, when the models are averaged, the RMSE improves because the resulting time series are smoother. In the wind climate sense, averaging does not necessarily improve the model biases.

3.4 WRF setup

We make a first attempt to examine whether using an ensemble of simulations combining multiple physics, land initial conditions and re-initialization strategy can be used to reliably estimate the uncertainty of the wind resource.

In Table 1 are the various parameters modified among the simulations. We use three different PBL schemes: the Mellor-Yamanda (MYJ) scheme (Janjic, 2001), the MYNN scheme (Nakanishi and Niino, 2006) and the YSU scheme (Hong et al., 2006). The soil moisture in the simulations is initialized from the same source as the atmospheric initial conditions (e.g. ERA Interim; Dee et al., 2011b) or from the Global Land Data Assimilation system (LGDAS, Rodell and et al, 2004). Lastly, the model re-initialization strategy is varied. The "10D" simulations are initialized at 00:00 GMT and run for 11 days, disregarding the first 24 hours; the "1D" simulations are initialized at 12:00 GMT and run for 36 hours, disregarding the first 12 hours.

Run name	PBL scheme	soil moisture source	simulation length (days)
MYJ-G	MYJ	GLDAS	10
MYJ	MYJ	ERA	10
MYJ-D	MYJ	ERA	1
MYN-G	MYNN	GLDAS	10
MYN	MYNN	ERA	10
MYN-D	MYNN	ERA	1
YSU-G	YSU	GLDAS	10
YSU	YSU	ERA	10
YSU-D	YSU	ERA	1

Table 1. Description of various WRF simulations

The simulations were carried out for a domain over South Africa as part of the Wind Atlas of South Africa (WASA) project for the one period from 1 June 2012 to 31 May 2013. We choose this domain and period because as part of the WASA project provides a high-quality set of observations, which are currently not available for an European domain. The stations used for validation are described in Mortensen et al. (2014). The domain (with a horizontal grid spacing of 45, 15 and 5 km) and the location of the sites is shown in Fig. 3. The 10 masts are equipped with identical instrumentation where the top-most anemometer is at a height of between 61.5 and 62 m AGL.

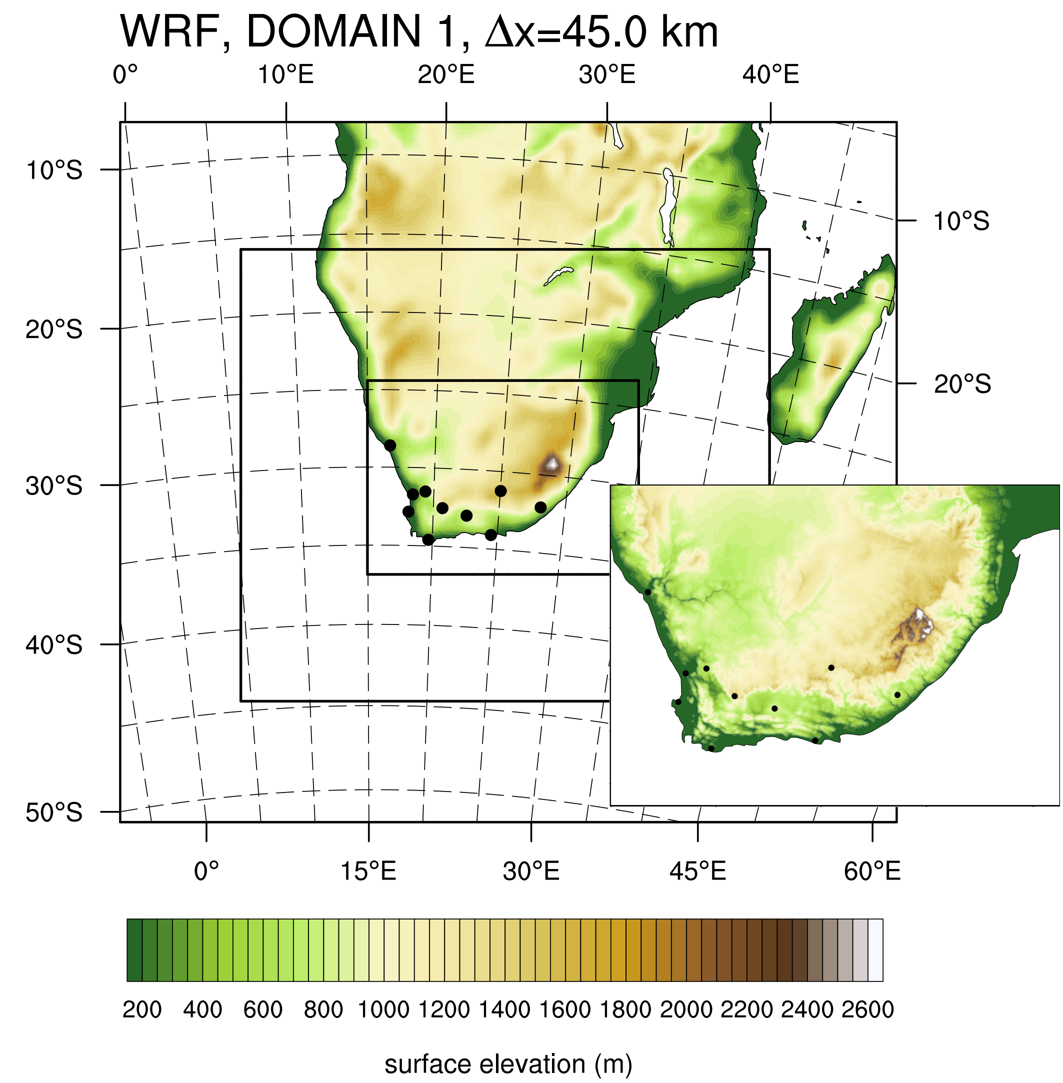

Figure 3. Surface elevation (m) and domain configuration used in the WRF simulations. The black dots indicate the position of the 10 validation masts (WM01–WM10). The inset shows the surface elevation of the inner domain.

3.5 Results

Verification at sites

Figure 4 shows the mean bias in wind speed as defined

$$\text{Error} = (\overline{U}_{WRF} - \overline{U}_{OBS}) \tag{1}$$

$$\text{Relative Error} = (\overline{U}_{WRF} - \overline{U}_{OBS})/\overline{U}_{OBS}, \tag{2}$$

where $\overline{U}_{WRF}$ and $\overline{U}_{OBS}$ are the mean wind speed simulated by WRF and observed, respectively, at each of the sites. Positive errors mean that the WRF model overestimates the mean wind speed at the site. The observed means are computed as the simple arithmetic mean of the wind speed over all available measurements during the period 1 June 2012 to 31 May 2013. The WRF model estimate is obtained by direct downscaling of the inner grid (5 km horizontal resolution) model output to the site by the method described in Hahmann et al. (2017). Missing periods in the observations are removed from the time series of WRF model wind speeds, so that both samples are of equal size.

Figure 4 shows the errors and relative errors in mean wind speed at the height of the top anemometer (61.4–62 m) for the WRF output downscaled to each site, respectively. The errors are for all 9 simulations and 10 tall mast sites. The absolute errors are $<1\,\mathrm{m\,s^{-1}}$ at all sites and all model configurations, except for the MYJ-G run at WM03, and $<0.4\,\mathrm{m\,s^{-1}}$ for the combined MAE at all sites. For a given site, the errors may vary considerable among the various simulations, but the MAE is almost indistinguishable among them.

Figure 5 shows another way to look at the errors in Fig. 4. The errors are presented as boxplots, where the red line and red box show the median and mean error, respectively. The box boundaries represent the lower (25%) and upper (75%) quartiles, and the whiskers the minimum and maximum values. Here it is possible to see that on average the relative errors are smaller and have the smaller spread in the MYNN-based experiments.

Finally we can combine the error statistics as a function of site. This is done in Figure 6, where the y-axis now displays the absolute value of the mean error to facilitate interpretation. Four of the five sites with the smallest error spread are also the sites with the smallest mean error (except for WM01). The other five sites with larger spread are also the five sites with larger absolute mean error.

Another encouraging characteristic of the distribution of the errors is apparent in Fig. 4. For each site the performance of each simulation varies from site to site. For example, the MYN-D is "worst" simulation at WM01, but one of the "bests" at WM08. This characteristic of the errors suggest that one model configuration might be most accurate under certain conditions but worse under others. Thus, it might be possible to optimize the combination of the results to create a more precise wind atlas and to use the model spread as a measure for uncertainty.

Ensemble mean and spread

From the mean wind speed of each ensemble simulation, $\overline{U}_i$, it is possible to compute and plot the ensemble mean, $\tilde{U}$, and the ensemble spread, $S_{\tilde{U}}$, defined as

$$\tilde{U} = \frac{1}{N}\sum_{i=1}^{N}\overline{U}_i \tag{3}$$

$$S_{\tilde{U}} = \sqrt{\sum_{i=1}^{N}\frac{(\overline{U}_i - \tilde{U})^2}{N-1}}, \tag{4}$$

where $N = 9$ is the total number of ensemble members. The ensemble spread is simply the standard deviation of the mean of the ensemble members.

Figure 7 shows the ensemble mean of wind speed at 100 m AGL for the 9 ensemble members.

Wind speeds are high ($\lesssim 8\,\mathrm{m\,s^{-1}}$) over many areas of elevated terrain (see Fig. 3) and over the sea. The map of the ensemble mean shows many interesting features, which do not directly correspond to areas of complex terrain or high winds. It remains to be verified if these patterns are correlated with areas of reduced or enhanced uncertainties.

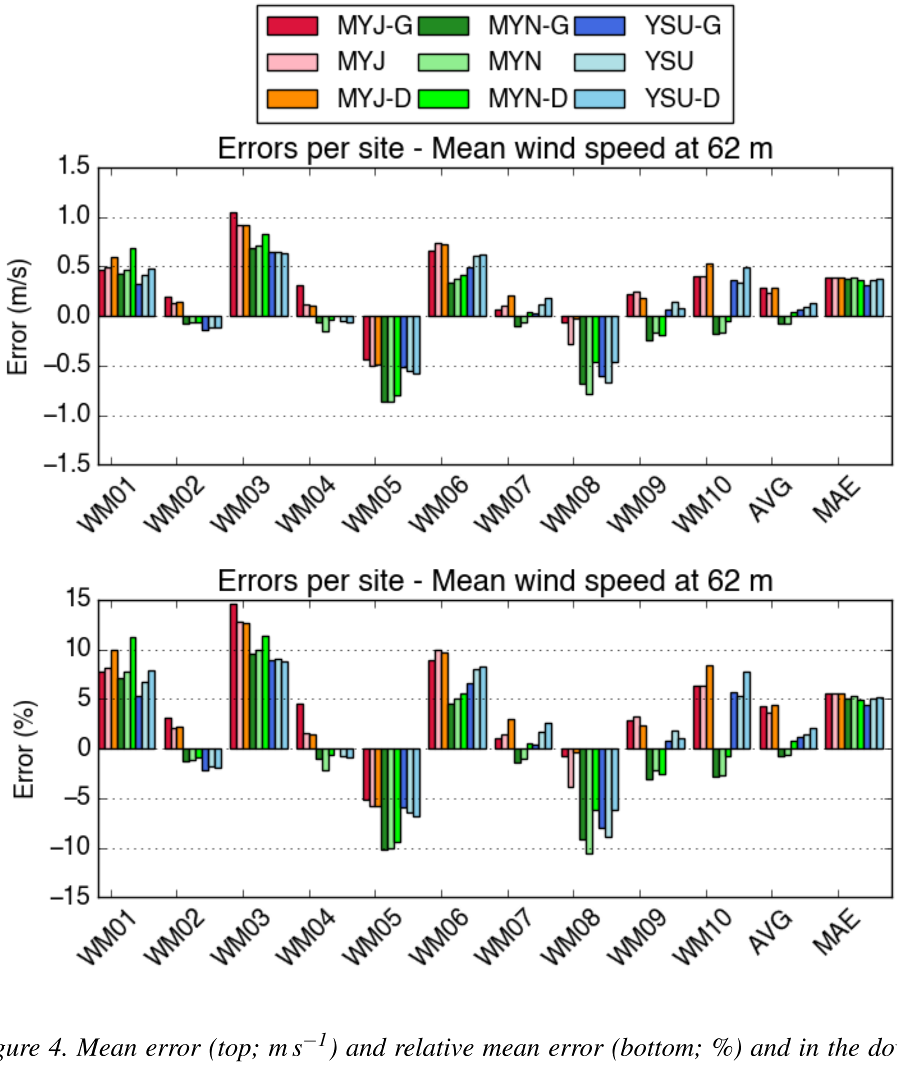

Figure 4. Mean error (top; $\mathrm{m\,s^{-1}}$) and relative mean error (bottom; %) and in the downscaled wind speed at about 62 m for each ensemble member in Table 1 for each of the 10 WASA sites. The last two sets of bars represent the mean error (AVG) and the mean absolute error (MAE) over all the sites.

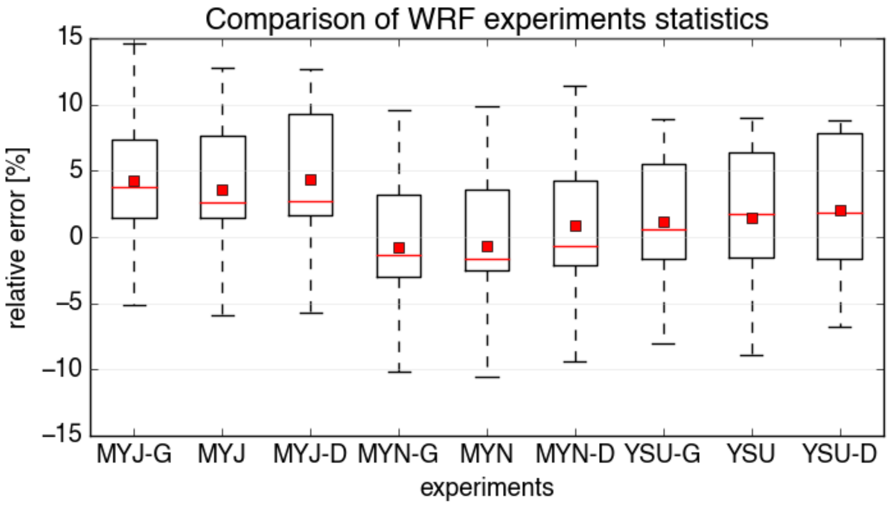

Figure 5. Comparison of statistics of the wind speed errors for each ensemble member in Table 1. The meaning of the box is as in regular boxplots: the red line and red box show the median and mean error, respectively. The box boundaries represent the lower (25%) and upper (75%) quartiles, and the whiskers the minimum and maximum values.

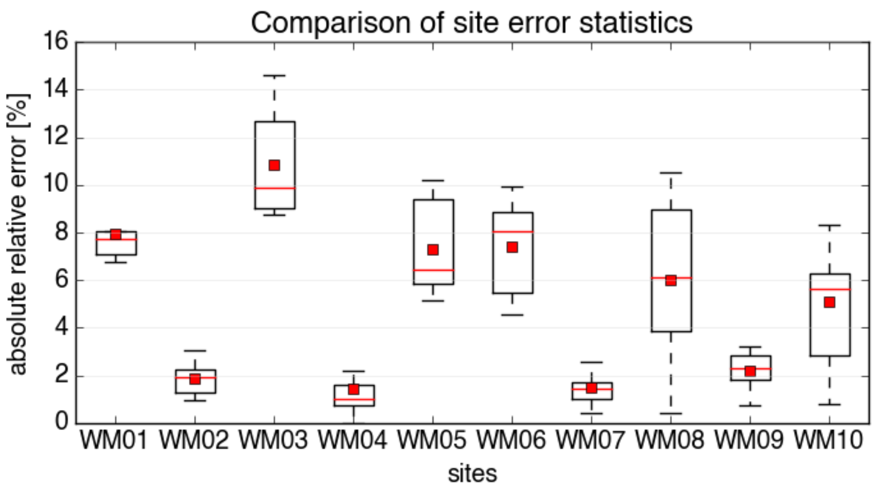

Figure 6. Comparison of statistics of the wind speed errors for each site of the various ensembles in Table 1. The meaning of the box is as in regular boxplots: the red line and red box show the median and mean error, respectively. The box boundaries represent the lower (25%) and upper (75%) quartiles, and the whiskers the minimum and maximum values.

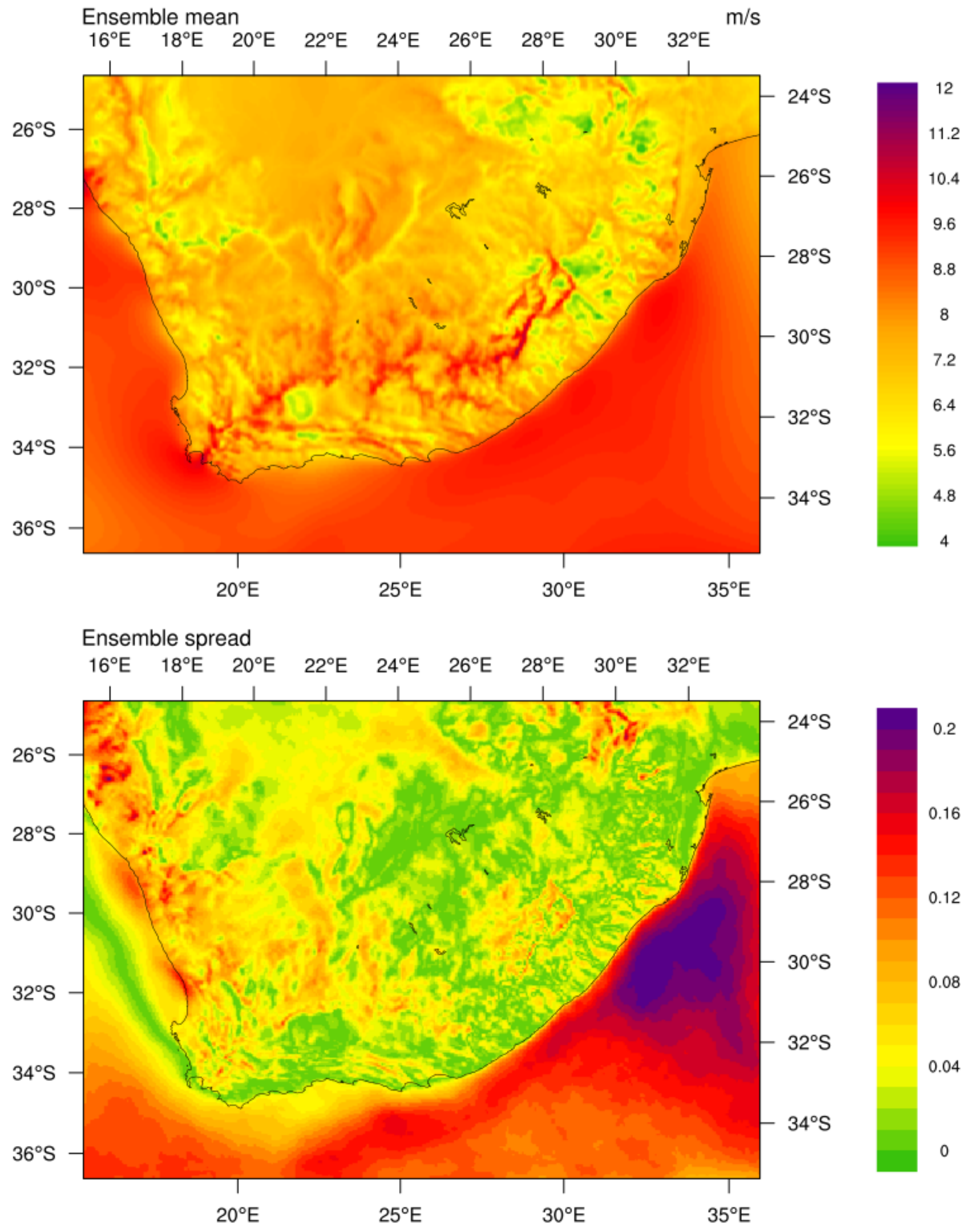

Figure 7. Top: Ensemble mean, $\tilde{U}$, and Bottom: ensemble spread, $S_{\tilde{U}}$, of the wind speed ($m\,s^{-1}$) at 100 m AGL for the period from 1 June 2012 to 31 May 2013.

3.6 Summary and discussion

We have performed a series of nine one year simulations with varied PBL schemes, simulation length and source of land surface conditions to explore the possibility of using an ensemble of runs to estimate the uncertainty of a wind resource map. The results of the simulations are encouraging, but further analysis of the results is necessary to quantify how useful they are.

The principal disadvantage of the use of the ensemble mean and spread of the simulations is that it can be misleading, and will not be the best estimate of the most accurate value and its uncertainty, if clusters of similar simulations outcomes exist, and the ensemble mean lies between those clusters. Therefore, it is vital to design an ensemble system where the ensemble members do not cluster around similar simulation outcomes. This is definitely not the case for the ensemble used in this report, because the errors do cluster as a function of PBL scheme (Fig. 4).

Since most ensembles using initial condition perturbations alone tend not to have enough spread, combined ensemble methods (i.e., a combination of perturbed initial conditions and physical parameterizations) should, at least theoretically, give better results in terms of covering all possible forecast outcomes.

3.7 Recommendations

We recommend to expand the ensemble members used in this study to:

- Use different reanalysis to initialize and nudge the WRF simulations, e.g. NOAA Climate Forecast System Reanalysis (CFSR) and Modern Era Retrospective-Analysis for Research and Applications (MERRA and MERRA2);
- Use the various ensemble members' output from the new reanalysis ERA5 (ECMWF, 2016), whose data products will include information about uncertainties, which will be provided for each parameter at 3-hourly intervals and at a horizontal resolution of 62 km.
- Find a method to quantify if two ensemble simulations are too similar and should be removed from the set;
- Identify potential statistical techniques (e.g. machine learning) to optimally combine the results from the various ensemble members into a single wind resource map.

4 Mesoscale sensitivity experiments in the NEWA project

The setting up of the optimum WRF configuration for wind assessment is not a straightforward task considering the large number of degrees of freedom in the configuration of the model as well as the input data. A systematic approach exploring all possible combinations of these configuration settings is not intended here. Instead, we will rather use the experience of the mesoscale modellers in NEWA to determine a few fundamental settings and strategies that are known to have the largest impact on the wind resource, leaving everything else fixed based on the experts consensus.

The objective is to come up with a first version of the unified WRF model for wind energy, which will be the baseline for further model development and evaluation activities in NEWA. As new changes are introduced, as a result of the model evaluation process, it will be possible to track this changes throughout the project with quantitative information about added performance.

The initial stage to setting up a unified model is to verify that all the modelers speak the same language when it comes to conducting simulations with WRF. Hence, this verification phase will make sure that the WRF implementation accurately represents NEWA's conceptual description of the model and the solution of the model. The focus is not to compare simulations with observations (validation) but to examine the relative difference among different model configurations compared to a baseline result.

The sensitivity analysis will also help ranking the importance of different WRF options in terms of their impact on the variability of variables of interest in different wind climate conditions.

4.1 WRF configuration

As an initial activity of the NEWA WP3, a series of sensitivity experiments were carried out for five European domains. Figure 8 shows the location of the outer 27 km WRF domain and the five inner 3 km domains.

The five sensitivity domains share an identical outer domain at 27 km, covering the area displayed in Figure 8, but were run independently by each modeling group. The locations and grid sizes for each domain are shown in Table 2.

Domain	Inner grid size	Grid center lat/lon
NE	316 × 244	56.85°N, 18.64°E
NW	337 × 343	53.77°N, 7.92°E
PE	244 × 244	38.98°N, 8.41°W
SW	196 × 196	43.11°N, 0.56°W
SE	508 × 328	38.94°N, 33.51°E

Table 2. Grid sizes and center latitude/longitude for the five inner WRF domains of the sensitivity experiments in Figure 2.

Six year-long WRF model experiments were conducted for each of the five domains. These are described in Table 3. The experiments were run using two PBL parameterizations, the YSU and MYNN schemes, and 3 integration methods, daily initialization (S1), seven days with spectral nudging only in the external domain (W1), and seven days with spectral nudging in all domains (W3). In the S1 runs, initialized at 00:00 GMT, the first 12 hours of the simulations were disregarded, in the W1 and W3 simulations, initialized at 12:00 GMT, the first day was disregarded. Besides PBL scheme and the use of spectral nudging, all other namelist options are identical

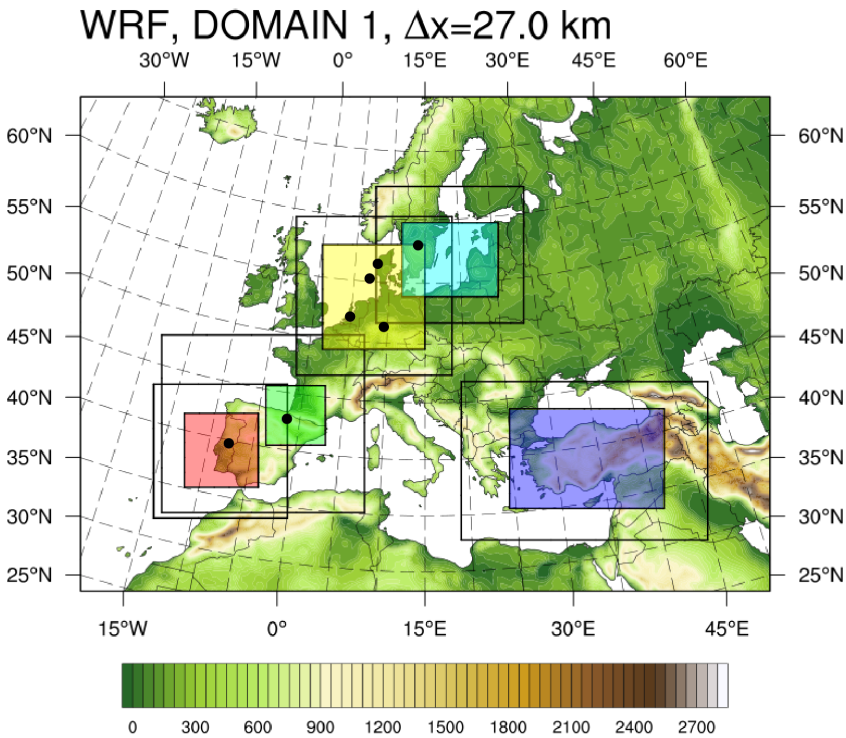

Figure 8. The five WRF model domains used in the model sensitivity experiments: NE (turquoise), NW (yellow), PE (red), SW (green) and SE (purple).

PBL scheme	YSU	MYNN
Daily	MYNL61S1	YSUL61S1
Weekly nudge D1	MYNL61W1	YSUL61W1
Weekly nudge D1–D3	MYNL61W3	YSUL61W3

Table 3. The six WRF model sensitivity experiments

among the simulations. These are summarized in Table 4. A complete namelist for experiment MYNL61S1 in NW is included in Appendix A.

The runs cover the period of 1 January to 31 December 2015, and were run using the ERA-Interim (Dee et al., 2011a) forcing data and Optimal Interpolation (Reynolds et al., 2002) sea surface temperatures and sea-ice concentrations. Most other details of the simulations, including common parameterizations, are listed in Table 4.

4.2 Summary of sensitivity experiments results

A long description of all the results of the sensitivity experiments is beyond the scope of this report, but a short summary is provided here. A presentation with many of the results discussed here is available in a separate Appendix.

The comparison of the results of the various simulations show that:

- Over water at 25 m AMSL annual mean wind speeds simulated in the MYNL61S1 run are often larger than those in the YSUL61S1 run, except for low-wind areas in the Mediterranean Seas (French Riviera and Turkey). Differences can be as large as $0.5 \mathrm{m\,s^{-1}}$ in the Baltic and Southern Portugal. At 100 m AMSL, a similar, but much reduced in magnitude, pattern is seen. The pattern of differences is almost identical when comparing the

WRF version	3.6 with bug fixes
Model levels	61 from surface to 50 hPa
Microphysics	WRF Single-Moment 5-class scheme (4)
Longwave Radiation	RRTMG scheme (4)
Shortwave Radiation	RRTMG shortwave (4)
Land Surface	Noah Land Surface Model (2)
Surface Layer	MM5 similarity (1) or MYNN (5)
Cumulus Parameterization	Kain-Fritsch scheme (1) on D1 and D2
Land	CORINE land surface data
	Constant surface roughnesses over land
Lakes	Water temperature of lakes from ERA-Interim
SST	OISST, updated daily
Forcing	ERA Interim pressure data
Grid nudging	Spectral nudging (2)
Constant	0.0003 s^{-1}
Level	No PBL (u and v) and above level 20
Wave number	15 and 11 in D1, varying values in D2 and D3.
Diffusion	Simple diffusion (option 1)
	2D deformation (option 4)
	6th order positive definite numerical diffusion (option 2)
	rates of 0.06, 0.08, and 0.1 for D1, D2, and D3
	vertical damping.
Advection	Positive definite advection of moisture and scalars.
Nesting	one way
Relax zone	4 points

Table 4. Common model setup and parameterizations used in the sensitivity experiments.

MYNL61W1 and YSUL61W1 runs.

- Over land at a height of 100 m, the wind speed simulated using the YSU scheme is larger than that using the MYNN scheme. The pattern and magnitude of this differences collocated and related to the underlying surface roughness length (Figure 9).
- The simulations show very interesting patterns in the frequency of stability conditions. These are derived from the surface-layer Monin-Obukov stability parameter, L, that is a model output field in the simulations. The maps show that:
  - Stable conditions (i.e., $1/L > 0.005\,\mathrm{m}$) are common over land, specially in the three southern domains and can reach over 50% of the time in mountainous areas in Turkey and the Pyrenees.
  - Unstable conditions (i.e., $1/L < -0.005\,\mathrm{m}$) are found over the oceans, specially in the Atlantic and Mediterranean off the coast of France and Turkey. Some regions can reach 70%.
  - Neutral conditions (i.e., $|1/L| < 0.005\,\mathrm{m}$) occur in less than about 20% of the time in all regions. The largest areas are in the Baltic Sea and off the coast of Portugal.
- The simulations show systematic changes in the frequencies of stability classes between the MYNL61S1 and YSUL61S1 simulations:
  - The fraction of stable conditions decreases over land in all areas
  - The fraction of neutral conditions increases over land in all areas
  - The fraction of unstable conditions decreases over all areas, but specially over land, sometimes by as much as 20%.

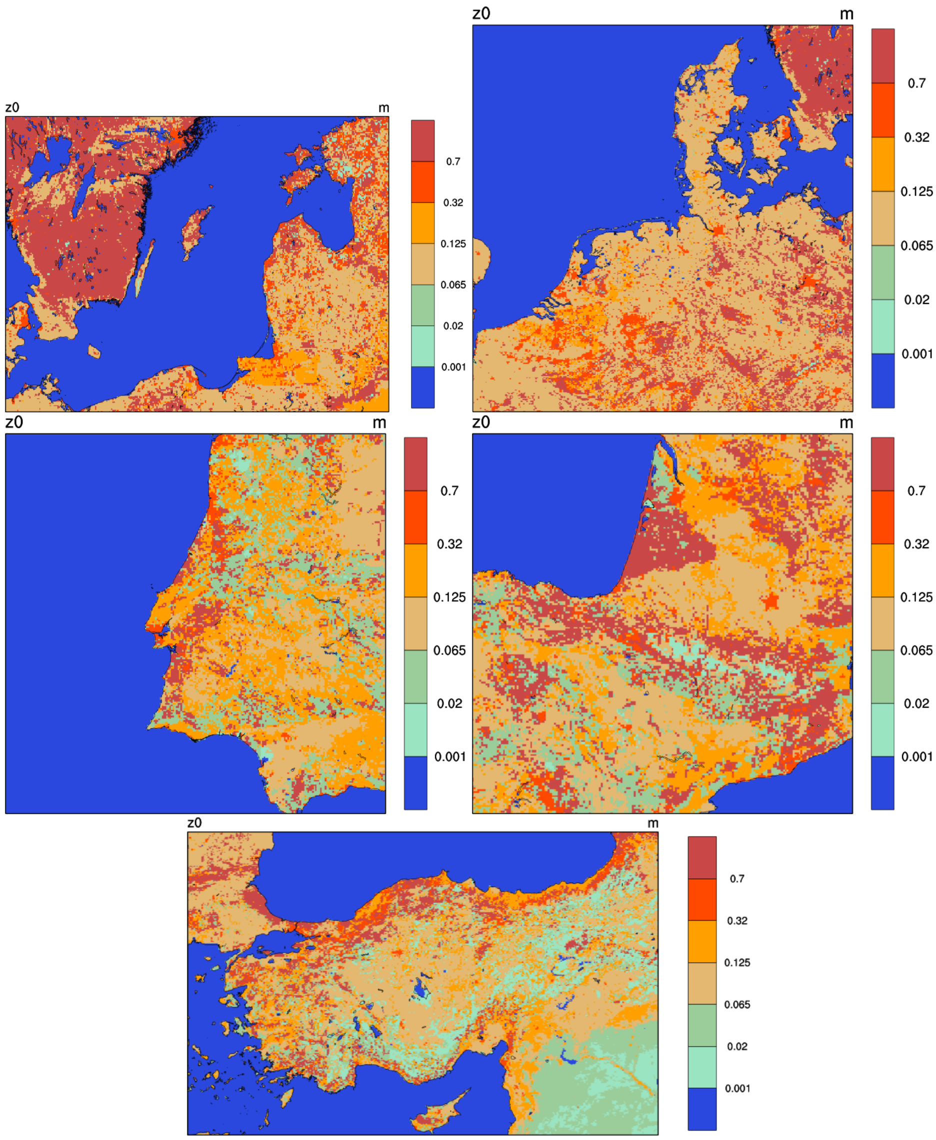

Figure 9. Surface roughness length (m) of the five 3 km × 3 km domains of the NEWA sensitivity experiments.

- The standard deviation of the hourly wind speed at 100 m AGL shows high values over water ($> 4.5 \mathrm{m\,s^{-1}}$) over the North, Aegean and Baltic Sea and over complex terrain over Turkey and the Pyrenees.
- The ratio of the hourly wind speed variance between the MYNL61S1 and YSUL61S1 simulations shows mostly values less than one (max of about 0.75) over land, which again seem to be collocated with forest regions.
- The ratio of the hourly wind speed variance between the daily MYNL61S1 and weekly MYNL61W1 nudged simulations shows a decrease in variance at 100 m AGL everywhere as expected, but the values are only mostly below 0.9 and without a particular preference for land or terrain except for the Pyrenees and Southern France, with somewhat larger values (max 0.8). Unfortunately the SE simulation was performed without activating the spectral nudging and thus shows larger variance values than the S1 simulation.

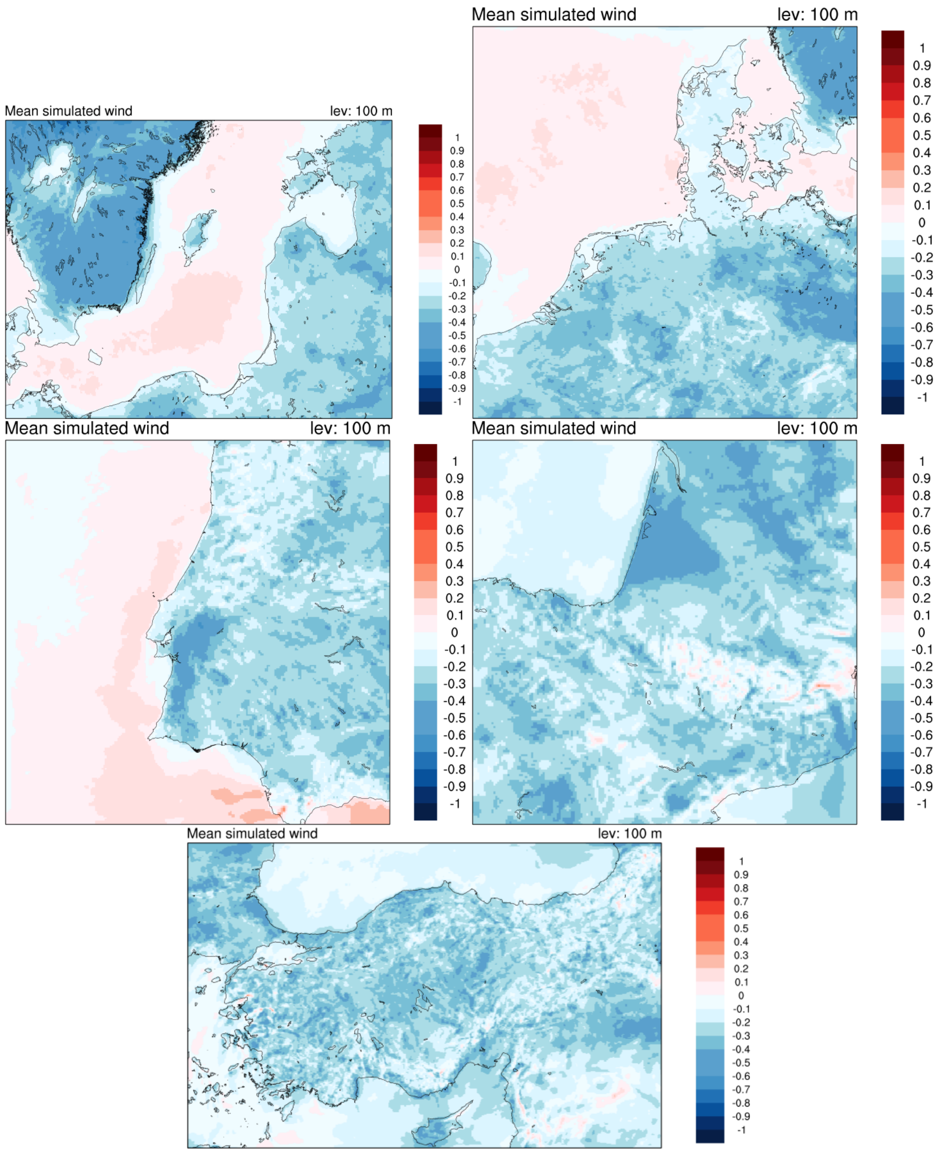

Figure 10. Differences in annual mean wind speed ($m\,s^{-1}$) during 2015 at 100 m between the MYNL61S1 and YSUL61S1 simulations for the five simulated areas.

5 Wind resource assessment with the Analog Ensemble method

5.1 Introduction

Another method to generate uncertainty information of the wind resource is the Analog Ensemble (AnEn) concept which was proposed by Hamill and Withaker (2006) and Delle Monache et al. (2013). The original purpose of the AnEn method was to generate an uncertainty forecast from a purely deterministic short-term weather prediction. The uncertainties are estimated by comparing past observations with corresponding past forecasts (analogs) which are most similar to a current deterministic forecast.

The AnEn concept was adapted for wind resource assessment by Vanvyve et al. (2015). Long-term historical data are compared with wind speed observations from a shorter time period. By finding analogs in the training period, missing data (e.g. wind speed observations) for specific sites can be reconstructed. Vanvyve et al. (2015) showed that the AnEn requires only a minimum of about a year of mast measurements and long-term historical wind data such as reanalyses or observations from nearby long-term weather station records. It was shown that the AnEn method is an efficient stand-alone technique that can replace existing methods for estimating the long-term wind resource at a target site and that it is particularly well-suited to handle difficult sites, e.g. in complex terrain.

Previous studies did not optimize the predictor selection but assigned equal weights to each predictor variable and neglected the strength of the relationships between individual predictors and the variable to be predicted (Delle Monache et al., 2013; Alessandrini et al., 2015; Vanvyve et al., 2015). Junk et al. (2015) proposed an algorithm which finds the optimal predictor weights by minimizing the Continuous Ranked Probability Score (CRPS) over all possible combinations. For probabilistic wind power forecasting it was shown that an optimization of predictor weights can significantly improve the skill of the AnEn.

The AnEn for wind resource assessment is also a very useful method for the NEWA wind atlas. It can be applied to generate uncertainty information for the wind atlas and to extend the high-resolution data set in case the computational resources are not sufficient to generate a 30 year high-resolution wind atlas. We performed several test studies to evaluate the potential of the AnEn method in the context of NEWA which are described and discussed in the following.

A similar method for the long-term extrapolation of wind measurements is the Measure-Correlate-Predict (MCP) method which is widely used by the wind industry (Rogers et al., 2005). The MCP method requires a good correlation between wind measurements and historical wind data as well as homogeneity in the historical data set which is often not the case. Furthermore it relies on wind speed and direction only, in contrast to the AnEn which can consider additional predictors.

The strengths of the AnEn method are (Vanvyve et al., 2015):

- Good quality of results, i.e. the reconstructed long-term wind resource is well correlated with on-site wind observations
- It yields a wind resource frequency distribution with uncertainty bounds based on actual physical processes
- It only requires long-term reanalysis data and observations (typically 1–4 years) which do not necessarily need to be well correlated
- It requires very small computational resources

5.2 Description of the AnEn method

The purpose of the AnEn method for wind resource assessment is to reconstruct the time series of wind speed at a target site for a period in which there are no observations are available. For every point in time of the period to be reconstructed the following steps are performed (see also Fig. 2 in Vanvyve et al. (2015)):

1. **Retrieve historical data** for that point (e.g. from reanalysis data): Retrieve the values of different predictors and use a time window (e.g. 2 hours) around the point of interest to capture trends.
2. **Find analogs in the training data set**: Search the training data set (both reanalysis data and observations available) for cases with conditions similar to the conditions of the point to be reconstructed (based on the values of the predictors), the same time window as in step 2 is applied to capture trends.
3. **Select the best analogs** for every point to be reconstructed.
4. **Retrieve the corresponding observed values**: They constitute the analog ensemble for the point to be reconstructed.

The result is an analog ensemble for every point in time of the reconstructed period.

5.3 Evaluated sites and test cases

We tested the AnEn for wind resource assessment for 7 sites with available met mast data (see Fig. 11). The sites include onshore masts in flat (Hamburg, Cabauw) or slightly complex terrain (Falkenberg, Karlsruhe) as well as offshore masts. As historical data set we used MERRA reanalysis data. For the tests we used a rather short training period of 3 months with overlapping measurements and reanalysis data and reconstructed the measurements for the previous 9 months which we then compared with the actual measurements for that period. Ideally, the training period should be at least one full year to include every season. In the basic setup 4 equally weighted predictors were used: wind speed and wind direction in 50 m height, sea level pressure and temperature in 2 m height. For every hour to be reconstructed the 50 best matching analogs were selected. A number of test cases have been studied (details listed in Table 5) in which the effect of the numbers of predictors and analogs on the results has been analyzed (case 1–3). Subsequently, the observational data set has been replaced by mesoscale model data (case 4). Each case was initially run with equal predictor weights and then repeated with optimized predictor weights derived from the algorithm developed by Junk et al. (2015). To make the computations feasible, the number of analogs was reduced in the cases with the optimization algorithm.

Figure 11. Locations of the evaluated test sites.

case	number of analogs	number of predictors	predictor weighting	historical data	observed data
1a	50	4	equal	MERRA	met mast
1b	20	4	optimized	MERRA	met mast
2a	150	4	equal	MERRA	met mast
2b	60	4	optimized	MERRA	met mast
3a	50	8	equal	MERRA	met mast
3b	20	8	optimized	MERRA	met mast
4a	50	4	equal	MERRA	WRF
4b	20	4	optimized	MERRA	WRF

Table 5. Details of the Analog Ensemble test cases.

5.4 Results

The skill of the AnEn method for the particular test cases was evaluated by comparing the reconstructed time series with the actual measurement data by means of the following measures:

- Continuous Ranked Probability Score (CRPS)
- Root Mean Square Error (RMSE)
- Bias
- Correlation coefficient (CORR)

The results in terms of these measures for the first test cases (1a and 1b) are shown in Table 6. The results are very satisfactory with CRPS mostly below 1.0, RMSE values below 2.0, high correlations around 90% and very low bias. Using optimized predictor weights improves the results slightly. In general, CRPS and RMSE are lower onshore than offshore. On the other hand, the correlation is higher for the offshore sites and lower for the most complex site Karlsruhe. To visualize the results of the AnEn, the wind speed distributions (PDF) of the AnEn, the actual observations and the reanalysis data are plotted in Fig. 12. The PDFs show a generally good agreement between reconstructed and original data. The AnEn outperforms the reanalysis data especially at the offshore sites and at Cabauw. At the other sites, the reanalysis data is already quite close to the observations but is still outperformed by the AnEn.

site	CRPS		RMSE		CORR		BIAS	
	equal	optimized	equal	optimized	equal	optimized	equal	optimized
Cabauw	0.90	0.79	1.60	1.41	87.67	90.19	-0.03	-0.02
Fino 2	1.22	1.06	2.13	1.88	88.49	91.08	0.21	0.16
Fino 3	1.21	1.02	2.11	1.82	89.32	91.90	0.10	0.10
Falkenberg	0.81	0.74	1.43	1.31	83.86	86.34	0.07	0.03
Hamburg	0.87	0.77	1.53	1.37	85.59	88.30	-0.33	-0.30
Karlsruhe	0.91	0.86	1.62	1.53	75.58	78.63	0.01	0.06

Table 6. Results for test case 1.

The rank histograms displayed in Fig. 13 show a good statistical consistency of the analog ensemble for most of the sites. Only Hamburg shows a slight bias towards larger wind speeds which can also be seen in the wind speed distribution in Fig. 13 and in the negative bias (6).

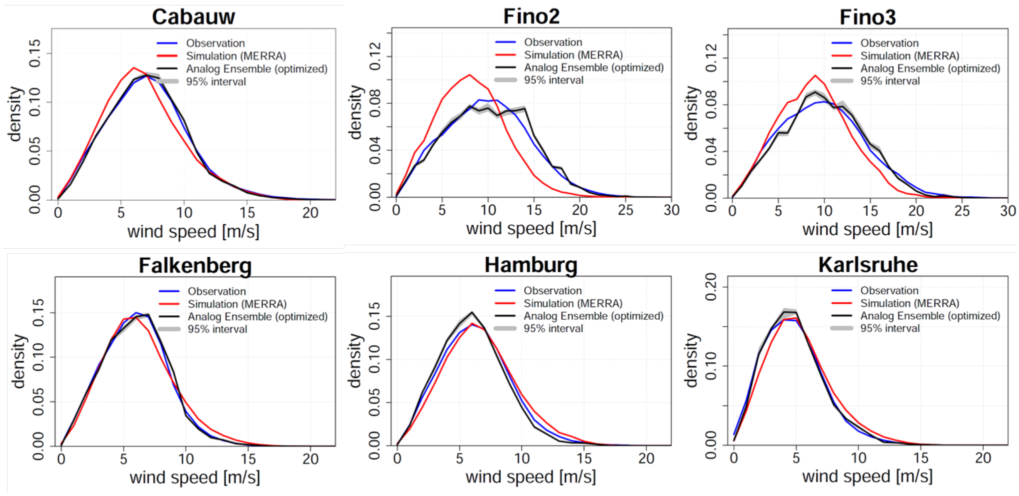

Figure 12. Wind speed distributions for test case 1.

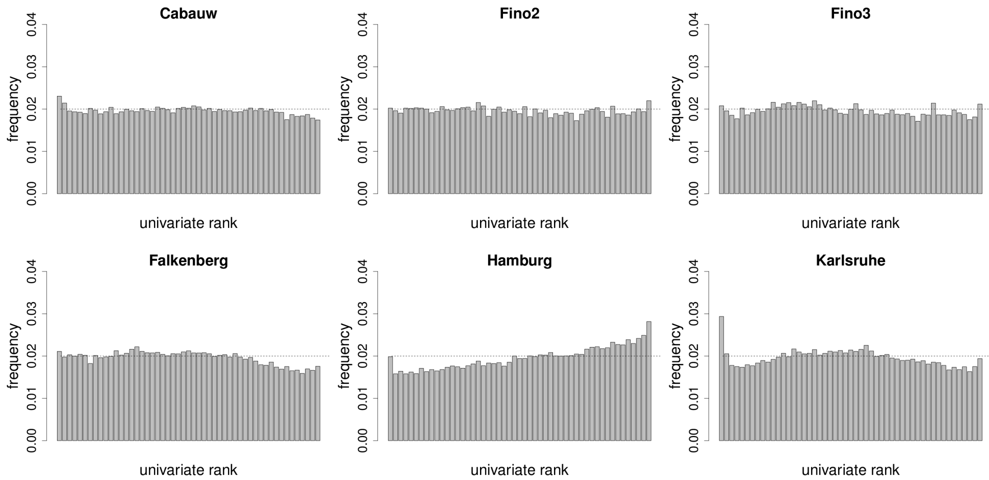

Figure 13. Rank histograms of the optimized analog ensemble for test case 1.

In the second test case the number of analogs was tripled to 150 with equal predictor weights and 60 with optimized predictor weights while keeping all other parameters the same. The results are almost identical compared to the first test case. This confirms results of a previous sensitivity study, shown in Fig. 14, where the number of analogs was varied between 2 and 50. Accordingly, about 20 AnEn members appear to be sufficient, the quality of results does not improve significantly using more analogs.

In the second test case, the number of predictors was doubled, adding wind speed and direction in 10 m and 2 m height, keeping the number of analogs constant at 50 (20 with optimized predictor weights). Doubling the number of predictors leads to an almost 50-fold increase in possible combinations and computational costs for the optimization algorithm. The results for the equal weighted predictors are improved, e.g. the CRPS and RMSE are about 5–10% lower and the correlation increased by about 0.02. However, there are virtually no improvements in the case with optimized predictor weights.

So far, observations have been used to train the AnEn. Within the NEWA wind atlas, the AnEn could also be used to extend the modelled time series at each grid point of the mesoscale model

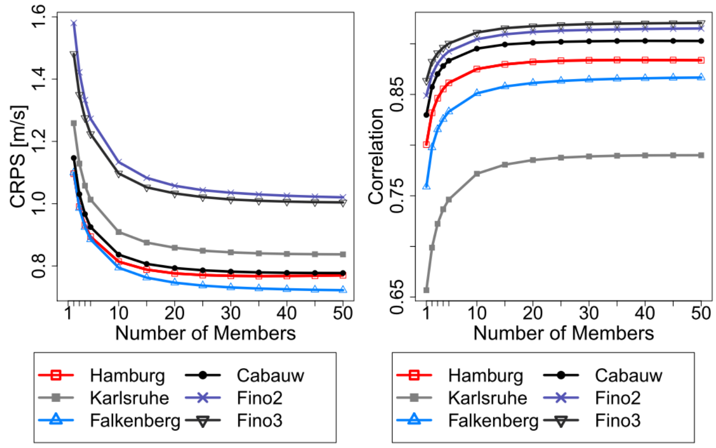

Figure 14. Sensitivity to the number of analogs.

to derive statistics for a longer time period than can be simulated. Furthermore, uncertainty information is provided by the AnEn. To check the skill of the AnEn for this purpose, we performed a preliminary study (case 4 in Table 5) where we replaced the observational training data by model output obtained with the mesoscale model WRF which is also intended to be used for generating the NEWA wind atlas. For the period of investigation the only available data at ForWind was for the location of FINO 1 (cf. Fig. 11). For this study, the four predictors and the number of analogs from the first test case have been used. As in the previous test cases, the training period was 3 months and the reconstruction period 9 months. WRF has first been driven by ERA-Interim data. In a second step, the study was repeated with MERRA data to obtain a harmonized setup as the AnEn used historical MERRA data as well.

Fig. 15 compares the wind speed distributions (PDF) of the AnEn (based on WRF), the actual observations and the reanalysis data. Furthermore the original WRF data is displayed. As expected, the higher resolved and more advanced WRF simulations follow the measurements more closely than the reanalysis data. The analog ensemble yields an improvement for some wind speed regimes, e.g. for low wind speeds less than $6\mathrm{m\,s^{-1}}$ and for high wind speeds greater than $15\mathrm{m\,s^{-1}}$. In the intermediate regime the ensemble often delivers worse results than the reanalysis data. The AnEn curve appears more ragged compared to the previous test cases. However, this could also be related to the different location of FINO 1 which was not evaluated in the previous test cases. The quality of the AnEn as assessed by the four measures defined above is even better than in the previous test cases (see Table 7), although a general conclusion cannot be drawn due to the different locations. Using MERRA instead of ERA-Interim data to drive WRF does not significantly improve the results.

forcing data	CRPS		RMSE		CORR		BIAS	
	equal	optimized	equal	optimized	equal	optimized	equal	optimized
ERA-Interim	0.93	0.82	1.61	1.43	93.64	95.22	0.20	0.37
MERRA	0.94	0.83	1.61	1.46	93.99	95.42	0.28	0.48

Table 7. Results for test case 4 (site: FINO1).

5.5 Conclusions and outlook

The Analog Ensemble for wind resource assessment is a well-suited and efficient tool to es-

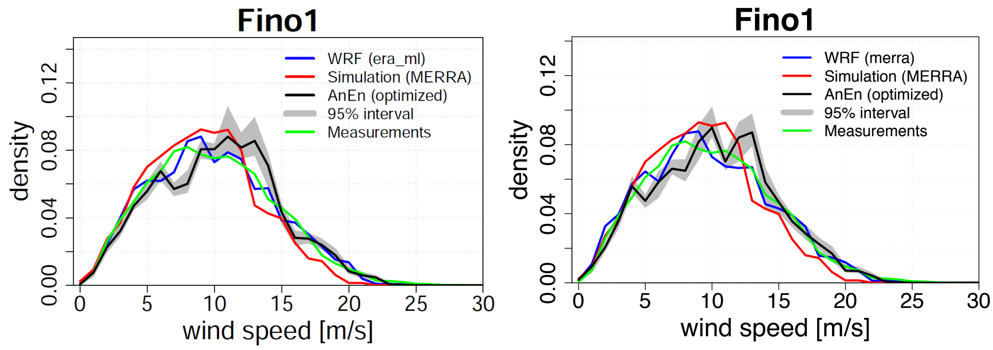

Figure 15. Wind speed distributions for test case 4, left: WRF driven by ERA-Interim, right: WRF driven by MERRA.

timate the long-term wind resource at sites with short-term measurement data. It outperforms existing methods like MCP as it is not dependent on a good correlation between observations and long-term reanalysis data and adds uncertainty information to the reconstructed time series.

We have tested the AnEn method for several onshore and offshore sites and could confirm that the AnEn method works and delivers results, which are very close to the actual observations and significantly better than the reanalysis data. The number of predictors and analogs can be kept small but optimizing the predictor weights improves the CRPS and RMSE by 5–10%.

A preliminary test with mesoscale model data instead of observations was successful, although further tests are necessary to prove that this concept is not only suitable to extend time series of measurement sites but also to extend the NEWA wind atlas to a longer time period and to provide uncertainty information for it. The next steps would be to repeat the analysis for land stations and complex terrain and to extend the training and reconstruction periods. Furthermore the method needs to be tested for different WRF setups.

Acknowledgements

The NEWA project counts with the support from an ERA-Net Plus consortium composed by the European Commission and 9 funding agencies from 8 member states:

- Public Service of Wallonia, Department of Energy and Sustainable Building (Belgium)
- Department of Economy, Science and Innovation Flemish Government (Belgium)
- Danish Energy Authority (Denmark)
- Federal Ministry for the Economic Affairs and Energy, on the basis of the decision by the German Bundestag (Germany)
- Latvijas Zinatnu Akademija (Latvia)
- Funda cão para a Ciência e a Tecnologia (Portugal)
- Ministerio de Econom'a y Competitividad (Spain)
- The Swedish Energy Agency (Sweden)
- The Scientific and Technological Research Council of Turkey (Turkey)

References

Al-Yahyai, S., Y. Charabi, A. Al-Badi, and A. Gastli, 2012: Nested ensemble NWP approach for wind energy assessment. *Renew. Energy*, **37**, 150–160.
URL http://dx.doi.org/10.1016/j.renene.2011.06.014

Alessandrini, S., L. Delle Monache, S. Sperati, and J. Nissen, 2015: A novel application of an analog ensemble for short-term wind power forecasting. *Renewable Energy*, **76**, 168–781.

Berner, J., S.-Y. Ha, J. P. Hacker, A. Fournier, and C. Snyder, 2011: Model Uncertainty in a Mesoscale Ensemble Prediction System: Stochastic versus Multiphysics Representations. *Mon. Weather Rev.*, **139**, 1972–1995.
URL http://journals.ametsoc.org/doi/abs/10.1175/2010MWR3595.1

Buizza, R., P. L. Houtekamer, G. Pellerin, Z. Toth, Y. Zhu, and M. Wei, 2005: A Comparison of the ECMWF, MSC, and NCEP Global Ensemble Prediction Systems. *Mon. Weather Rev.*, **133**, 1076–1097.

Dee, D. P., E. Kaellen, A. J. Simmons, and L. Haimberger, 2011a: Comments on “Reanalyses Suitable for Characterizing Long-Term Trends”. *Bull. Amer. Meteor. Soc.*, **92**, 65–70.

Dee, D. P., S. M. Uppala, A. J. Simmons, P. Berrisford, P. Poli, S. Kobayashi, U. Andrae, M. A. Balmaseda, et al., 2011b: The ERA-Interim reanalysis: configuration and performance of the data assimilation system. *Q. J. R. Meteorol. Soc.*, **137**, 553–597.
URL http://doi.wiley.com/10.1002/qj.828

Delle Monache, L., F. A. Eckel, B. Nagarajan, and K. Searight, 2013: Probabilistic Weather Prediction with an Analog Ensemble. *Monthly Weather Review*, **141**, 3498–3516.

Draxl, C., A. N. Hahmann, A. Peña, and G. Giebel, 2014: Evaluating winds and vertical wind shear from WRF model forecasts using seven PBL schemes. *Wind Energy*, **17**, 39–55.

ECMWF, 2016: ERA5 reanalysis is in production.
URL http://www.ecmwf.int/en/newsletter/147/news/era5-reanalysis-production

Giorgi, F., C. Jones, and G. R. Asrar, 2009: Addressing climate information needs at the regional level: the CORDEX framework. *Bull. - World Meteorol. Organ.*, **58**, 175–183.

Hahmann, A. N., J. Badger, C. L. Vincent, M. C. Kelly, P. J. H. Volker, and J. Refslund, 2014: Mesoscale modeling for the wind atlas for South Africa (WASA) Project. Tech. rep., DTU Wind Energy.
URL http://orbit.dtu.dk/services/downloadRegister/107110172/DTU_Wind_Energy_E_0050.pdf

Hahmann, A. N., C. L. Vincent, A. Peña, J. Lange, and C. B. Hasager, 2015: Wind climate estimation using WRF model output: Method and model sensitivities over the sea. *Int. J. Climatol.*, **35**, 3422–3439.
URL http://dx.doi.org/10.1002/joc.4217

Hahmann, A. N., P. J. H. Volker, J. Badger, N. G. Mortensen, and D. C. J. Schillebeeckx, 2017: Generalization of wrf-derived wind climatologies for validation and coupling of mesoscale and microscale models. *Wind Energy Science*, **In preparation**.

Hamill, T. and J. Withaker, 2006: Probabilistic quantitative precipitation forecasts based on reforecast analogs: Theory and application. *Monthly Weather Review*, **134(11)**, 3209–3229.

Hong, S.-Y., Y. Noh, and Dudhia., 2006: A new vertical diffusion package with an explicit treatment of entrainment processes. *Mon. Wea. Rev.*, **134**, 2318–2341.

IPCC, 2013: Climate Change 2013: The Physical Science Basis. Contribution of Working Group I to the Fifth Assessment Report of the Intergovernmental Panel on Climate Change. Tech. rep., Cambridge University Press, Cambridge, United Kingdom and New York, NY, USA.

Janjic, Z. I., 2001: Nonsingular implementation of the Mellor-Yamada level 2.5 scheme in the NCEP Meso model. Tech. rep., National Centers for Environmental Prediction: Camp Springs, MD, USA.

Junk, C., L. D. Monache, S. Alessandrini, G. Cervone, and L. von Bremen, 2015: Predictor-weighting strategies for probabilistic wind power forecasting with an analog ensemble. *Meteorol. Z.*, **24(4)**, 361–379.

Kleczek, M. A., G.-J. Steeneveld, and A. A. M. Holtslag, 2014: Evaluation of the Weather Research and Forecasting Mesoscale Model for GABLS3: Impact of Boundary-Layer Schemes, Boundary Conditions and Spin-Up. *Boundary-Layer Meteorol.*, **152**, 213–243.

Lee, J. A., W. C. Kolczynski, T. C. McCandless, and S. E. Haupt, 2012: An objective methodology for configuring and down-selecting an NWP ensemble for low-level wind prediction. *Mon. Weather Rev.*, **140**, 2270–2286.
URL `http://journals.ametsoc.org/doi/abs/10.1175/MWR-D-11-00065.1`

Lorenz, E. N., 1969: The predictability of a flow which possesses many scales of motion. *Tellus*, **21**, 289–307.
URL `http://tellusa.net/index.php/tellusa/article/view/10086`

Mortensen, N. G., J. C. Hansen, and M. C. Kelly, 2014: Wind Atlas for South Africa (WASA) Western Cape and parts of Northern and Eastern Cape Observational Wind Atlas for 10 Met. Masts in Northern, Western and Eastern Cape Provinces. Tech. Rep. April, DTU Wind Energy.

Murphy, J. M., D. M. H. Sexton, D. N. Barnett, G. S. Jones, M. J. Webb, M. Collins, and D. A. Stainforth, 2004: Quantification of modelling uncertainties in a large ensemble of climate change simulations. *Nature*, **430**, 768–772.
URL `http://www.ncbi.nlm.nih.gov/pubmed/15306806http://www.nature.com/doifinder/10.1038/nature02771`

Nakanishi, M. and H. Niino, 2006: An improved mellor-yamada level-3 model: Its numerical stability and application to a regional prediction of advection fog. *Bound.-Layer Meteor.*, **119**, 397–407.

Palmer, T. N., 2001: A nonlinear dynamical perspective on model error: A proposal for non-local stochastic-dynamic parametrization in weather and climate prediction models. *Q. J. R. Meteorol. Soc.*, **127**, 279–304.
URL `http://doi.wiley.com/10.1002/qj.49712757202`

Reynolds, R. W., N. A. Rayner, T. M. Smith, D. C. Stokes, and W. Q. Wang, 2002: An improved in situ and satellite SST analysis for climate. *J. Climate*, **15**, 1609–1625.

Rodell, M. and et al, 2004: The global land data assimilation system. *Bull. Am. Meteorol. Soc.*, **85**, 381–394.

Rogers, A. L., J. W. Rogers, and J. F. Manwell, 2005: Comparison of the performance of four measure–correlate–predict algorithms. *Journal of Wind Engineering and Industrial Aerodynamics*, **93**, 243–264.

Sanz Rodrigo, J., R. Chávez Arroyo, P. Moriarty, M. Churchfield, B. Kosović, P.-E. Réthoré, K. Hansen, A. Hahmann, et al., 2017: Mesoscale to microscale wind farm flow modeling and evaluation. *Wiley Interdisciplinary Reviews: Energy and Environment*, **6**.

Skamarock, W. C., J. B. Klemp, J. Dudhia, D. O. Gill, D. M. Barker, M. G. Duda, X.-Y. Huang, W. Wang, et al., 2008: A Description of the Advanced Research WRF Version 3. Tech. Rep. NCAR/TN-475+STR, National Center for Atmospheric Research.

Stainforth, D. A., T. Aina, C. Christensen, M. Collins, N. Faull, D. J. Frame, J. A. Kettleborough, S. Knight, et al., 2005: Uncertainty in predictions of the climate response to rising levels of greenhouse gases. *Nature*, **433**, 403–6.
URL `http://dx.doi.org/10.1038/nature03301`

Takayabu, I., H. Kanamaru, K. Dairaku, R. Benestad, H. von Storch, and J. H. Christensen, 2016: Reconsidering the Quality and Utility of Downscaling. *J. Meteorol. Soc. Japan. Ser. II*, **94A**, 31–45.
URL `https://www.jstage.jst.go.jp/article/jmsj/94A/0/94A{_}2015-042/{_}article`

Vanvyve, E., L. Delle Monache, A. J. Monaghan, and J. O. Pinto, 2015: Wind resource estimates with an analog ensemble approach. *Renew. Energ.*, **74**, 761–773.


eUDP
Energiteknologisk udvikling og demonstration
Energimyndigheten
Latvijas Zinātņu akadēmija
Latvian Academy of Sciences
Wallonie
SPW
Service public de Wallonie
Supported by:
Federal Ministry for Economic Affairs and Energy
on the basis of a decision by the German Bundestag
EWI
GOBIERNO DE ESPAÑA
MINISTERIO DE ECONOMÍA Y COMPETITIVIDAD
FCT
Fundação para a Ciência e a Tecnologia
MINISTÉRIO DA CIÊNCIA, TECNOLOGIA E ENSINO SUPERIOR
TÜBİTAK